Neutron study of local environment effects and magnetic clustering in $Fe_{0.7}Al_{0.3}$†

J. W. Cable, L. David,* and R. Parra*
Solid State Division, Oak Ridge National Laboratory, Oak Ridge, Tennessee 37830
(Received 7 March 1977)

Ordered $Fe_{0.7}Al_{0.3}$ is ferromagnetic below 400 K but becomes paramagnetic on cooling below 170 K and then is mictomagnetic below 92 K. We have used neutron-scattering methods to probe the microscopic magnetic-moment distribution of this alloy. Diffuse scattering data show the presence of large ferromagnetic clusters throughout all of these ordered regions and that the bulk behavior results from intercluster coupling. The Bragg scattering data yield Fe moments for the different lattice sites that are consistent with, and provide refined moment values for, a previously suggested local environment model. The results are interpreted in terms of clustered regions of α-site Fe atoms with $n \geq 4$ and $n < 4$ Fe nearest neighbors.

INTRODUCTION

Ordered Fe_3Al is one of the first alloys for which a local environment effect on the magnetic moment of an atom was demonstrated.[1] In this structure, the Fe atoms on β sites have eight Fe nearest neighbors and the same room-temperature moment as in bcc Fe ($2.18\mu_B$), while those Fe atoms on α sites have four Fe and four Al nearest neighbors and moments of only $1.50\mu_B$. The ordered structure is retained to 32-at.% Al with the excess Al tending to occupy the β sites.[2,3] The magnetization decreases rapidly with this excess Al and beyond 30-at.% Al the system is no longer spontaneously ferromagnetic.[4,5] The magnetic behavior is anomalous in the 27- to 32-at.%-Al region where the magnetization actually decreases with decreasing temperature.[4,5] Furthermore, mictomagnetism[6] appears at low temperatures in this region as indicated by shifted hysteresis loops on field cooling and by sharp cusps in the low-field susceptibilities.[5] The 30-at.% alloy has a particularly unusual behavior in that the state of magnetic order changes from ferromagnetic to paramagnetic to mictomagnetic on cooling. Furthermore, the shape of the magnetization curves indicates the presence of superparamagnetic clusters in all of these ordered regions. This neutron study was undertaken to gain insight into this rather complicated behavior. Diffuse scattering measurements were made to characterize the moment distribution within the clusters and Bragg scattering measurements were made to further refine the magnetic-moment dependence on local environment.

DIFFUSE SCATTERING

Neutron diffuse-scattering measurements were made on a polycrystalline sample of $Fe_{0.7}Al_{0.3}$ kindly furnished to us by Professor P. A. Beck. This sample was brick shaped ($1 \times 2 \times 3$ cm) and had been homogenized at 1200 °C for 7 d and then heat treated at 440 °C to produce a high degree of long-range order. The diffuse intensity was measured with 4.43-Å unpolarized neutrons at sample temperatures from 10 to 500 K. Absolute cross sections were obtained by calibration with a standard V scatterer. Total cross sections in zero field and at selected temperatures are shown in Fig. 1. These exhibit a sharp increase

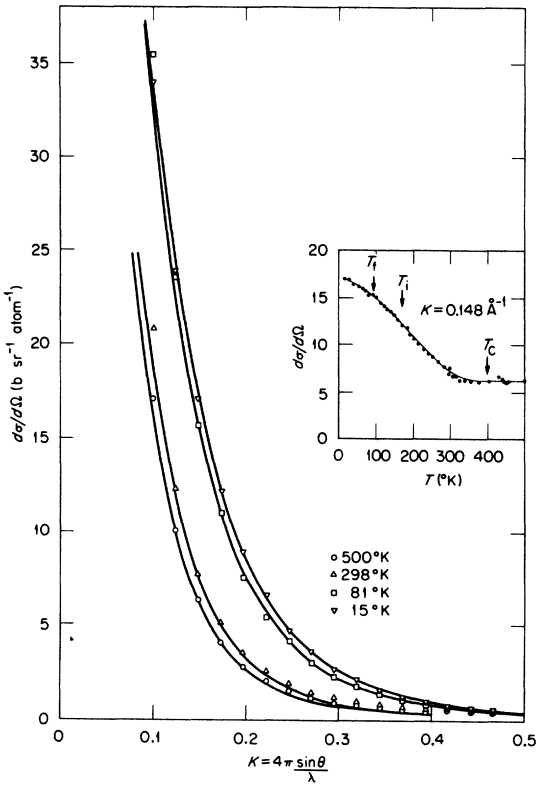

FIG. 1. Total cross sections of $Fe_{0.7}Al_{0.3}$ at selected temperatures. The inset shows the temperature dependence of $d\sigma/d\Omega$ at $K = 0.148$ Å and the transition temperatures indicated by bulk magnetization data (Ref. 5).

at small K indicating the presence of clustering. The strong temperature dependence of these cross sections, as illustrated in the inset for $K=0.148$ Å^{-1}, shows that most of this clustering is of magnetic origin. Remarkably, this is a continuous function without any anomalous behavior at the transition temperatures given by the magnetization data[5] and indicated by the labeled arrows in the inset. The magnetization data show that this alloy is ferromagnetic below $T_C=400$ K, paramagnetic below the inverse Curie temperature, $T_i=170$ K, and mictomagnetic below the freezing temperature $T_f=92$ K. These cross-section data show the presence of ferromagnetic clusters through all of these regions and that the ordering transitions result from the coupling of these clusters.

The clusters are spatially extended and, in the region of K space covered by this experiment, the neutrons "see" the clusters but not their relative orientations. Regardless of the ordered region then, the magnetic part of the cross section is approximately

$$\frac{d\sigma}{d\Omega}(K)=0.0484\,c^*[M(K)]^2 \qquad (1)$$

where c^* is the cluster concentration and $M(K)$ is the Fourier transform of the magnetic moment distribution within the cluster. In attempting to characterize the clusters, we find that $d\sigma/d\Omega^{-1/2}$ is linear in K^2 out to $K^2\simeq 0.15$ for the 15- and 81-K data and to $K^2\simeq 0.07$ for the 298- and 500-K data. This implies that the moment density decreases as $(1/R)e^{-\alpha R}$ at large R and that $M(K)=M(0)\alpha^2/(\alpha^2+K^2)$. The parameters $d\sigma/d\Omega(0)$ and α, obtained by least-squares fitting to the small-K data, are given in Table I and the corresponding cross sections are shown as the solid curves in Fig. 1. $(d\sigma/d\Omega)(0)$ has little, if any, temperature dependence but α increases (cluster radius decreases) with decreasing temperature.

There is some uncertainty about the nuclear and magnetic contribution to these total cross sections so that c^* and $M(0)$ are not obtained directly from $(d\sigma/d\Omega)(0)$. However, approximate values of c^* and $M(0)$ can be obtained for those clusters that are aligned in an applied magnetic field. We observed that about 33% of the small K cross section could be extinguished by a 12-kOe field at 214 K. This percentage of $(d\sigma/d\Omega)(0)$ at 298 K yields $c^*\times M(0)^2=464\mu_B^2$. The fundamental Bragg data give a magnetization of $0.430\mu_B$/atom at 220 K and 12 kOe. If this magnetization is taken as $c^*M(0)$, then one obtains $M(0)\simeq 1000\mu_B$ and $c^*\simeq 4\times 10^{-4}$. Thus there is a small concentration of large ferromagnetic clusters aligned by a 12-kOe field at 214 K. Since most of the cross section remains, there are also large ferromagnetic clusters that are not aligned.

TABLE I. Cross-section parameters for $Fe_{0.7}Al_{0.3}$ at selected temperatures.

T (K)	$\frac{d\sigma}{d\Omega}(0)$ (b sr^{-1} atom^{-1})	α (Å^{-1})
15	73	0.144
81	78	0.134
298	68	0.106
500	63	0.101

BRAGG SCATTERING

Bragg-scattering data were obtained for a pillar-shaped single crystal of approximate dimensions $1\times 1\times 10$ mm. This crystal was cut from the diffuse-scattering sample with a [110] direction parallel to the pillar axis. In the Fe_3Al type of order, Fe atoms preferentially occupy the α sites at 000, $\frac{1}{2}\frac{1}{2}\frac{1}{2}$ fcc and the β sites at $\frac{3}{4}\frac{1}{4}\frac{1}{4}$ fcc while the Al atoms tend to occupy the γ sites at $\frac{1}{4}\frac{1}{4}\frac{1}{4}$ fcc. There are three types of reflections with the nuclear structure factors:

$$F_{hkl}=\begin{cases}16\langle b\rangle; & h+k+l=4n,\\ 4(b_{\mathrm{Fe}}-b_{\mathrm{Al}})S; & h+k+l=4n+2,\\ 4i(b_{\mathrm{Fe}}-b_{\mathrm{Al}})S_{\beta\gamma}; & h+k+l=2n+1.\end{cases} \qquad (2)$$

Here, $\langle b\rangle=(1-c)b_{\mathrm{Fe}}+cb_{\mathrm{Al}}$, $S=2r_\alpha-r_\beta-w_\gamma$, and $S_{\beta\gamma}=r_\beta-w_\gamma$, where the r's and w's denote the fraction of the "rightly" or "wrongly" occupied lattice sites indicated by the subscripts. The fractional site occupations are determined from the identity, $2r_\alpha+r_\beta+w_\gamma=4(1-c)$, and the two long-range-order parameters, S and $S_{\beta\gamma}$.

Nuclear intensities were measured at room temperature in zero field with 1.07-Å unpolarized neutrons. Integrated intensities were obtained for the four or five innermost reflections of each type. These, corrected for the small magnetic components and for thermal motion, yield $F_{4n+2}/F_{4n}=0.242\pm 0.014$ and $F_{2n+1}/F_{4n}=0.120\pm 0.005$. With $b_{\mathrm{Fe}}=0.951$ and $b_{\mathrm{Al}}=0.3449\times 10^{-12}$ cm, these ratios correspond to $S=1.23\pm 0.07$, $S_{\beta\gamma}=0.607\pm 0.025$, $r_\alpha=1.01\pm 0.02$ (maximum $r_\alpha=1.00$), $r_\beta=0.70\pm 0.02$ and $w_\gamma=0.09\pm 0.02$. These fractional site occupations are consistent with those previously reported for the FeAl system.[1-3]

Magnetic structure factors were determined by the usual polarized-neutron flipping-ratio method. Such measurements yield magnetic to nuclear structure factor ratios which, for the three types of reflections, are given by

$$(F_M/F_N)_{4n}=\langle p\rangle/\langle b\rangle, \qquad (3)$$

$$(F_M/F_N)_{4n+2}=(2r_\alpha p_\alpha-r_\beta p_\beta-w_\gamma p_\gamma b_{\mathrm{Fe}}-b_{\mathrm{Al}})S, \qquad (4)$$

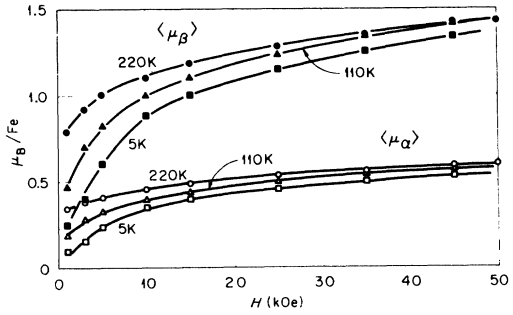

FIG. 2. Isothermal magnetization curves for the Fe moments at α and β sites.

and

$$(F_M/F_N)_{2n+1} = (r_\beta p_\beta - w_\gamma p_\gamma)/(b_{Fe} - b_{Al})S_{\beta\gamma}. \quad (5)$$

Here, $4\langle p\rangle = 2r_\alpha p_\alpha + r_\beta p_\beta + w_\gamma p_\gamma$ and the p's are the magnetic scattering amplitudes of Fe atoms on the subscripted lattice sites. These are related to the Fe moments by $p_i = 0.27\mu_i f$, where f is the form factor which is independent[1,7] of lattice site. Since the site occupations, long range order parameters and form factors[7] have all been determined, the μ_i's are directly obtained by appropriate combinations of these F_M/F_N ratios for the three types of reflections.

F_M/F_N ratios for the (220), (002), and (111) reflections were measured as a function of applied field at 220 K (ferromagnetic region), 110 K (paramagnetic region), and 5 K (mictomagnetic region). Here, the mictomagnetic state was developed by cooling in a remanent field of ~580 G. The magnetic moments of Fe atoms on α and β sites obtained from these ratio are shown as a function of applied field in Fig. 2. Even though these moment values are for particular lattice sites, they should be regarded as average values since the number of nearest-neighbor Fe atoms and therefore the moment, at a given type of lattice site may vary. Accordingly, the moments are given as averages, $\langle\mu_\alpha\rangle$ and $\langle\mu_\beta\rangle$. The uncertainty in these values is about 1% for $\langle\mu_\alpha\rangle$ and about 4% for $\langle\mu_\beta\rangle$. The largest γ-site moment obtained ($\langle\mu_\gamma\rangle = -0.28\mu_B$) is considerably smaller than the β-site moments even though both sites have eight Fe nearest neighbors ($r_\alpha = 1.0$). However, the low γ-site Fe occupancy ($w_\gamma = 0.09 \pm 0.02$) results in a large uncertainty (~90%) in $\langle\mu_\gamma\rangle$. We therefore confine our attention to the α- and β-site moments. These exhibit the same H and T dependence as the bulk magnetization with Brillouin-type isothermal magnetizations that decrease in magnitude with decreasing temperature. An Arrott plot for the α-site moments is shown in Fig. 3. This plot shows a spontaneous α-site moment at 220 K but not at the lower temperatures in agreement with the bulk magnetization data. Spontaneous moments were obtained by a linear extrapolation of the low-H/μ data and saturation moments were taken from a linear $1/H$ extrapolation of the high-field data. These are given in Table II.

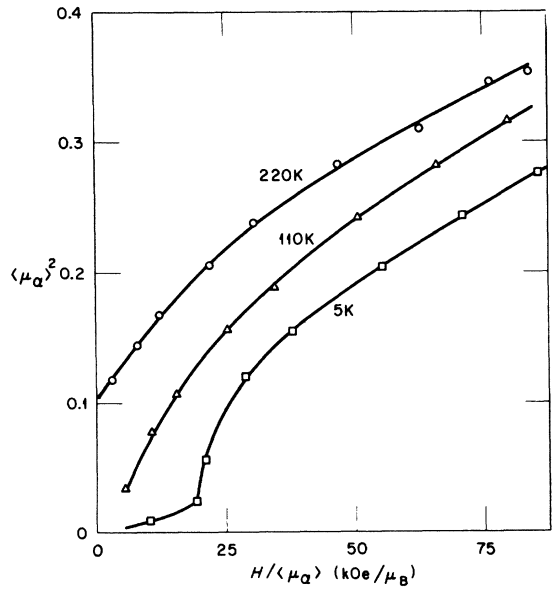

FIG. 3. Arrott plots for the α-site Fe moments showing spontaneous magnetization at 220 K but not at the lower temperatures.

TABLE II. Spontaneous and saturation moments for $Fe_{0.7}Al_{0.3}$.

T (K)	$\langle\mu_\alpha\rangle_0$	$\langle\mu_\alpha\rangle_\infty$	$\langle\mu_\beta\rangle_0$	$\langle\mu_\beta\rangle_\infty$
220	0.324	0.656	0.780	1.57
110	0	0.646	0	1.62
5	0	0.613	0	1.56

DISCUSSION

The rapid decrease in magnetization of the ordered Fe-Al alloys between 25- and 32-at.% Al is clearly associated with the introduction of Al atoms onto β sites. This fact, along with the neutron observation[1] of a reduced α-site moment in Fe_3Al and the Mössbauer observation[8] of three hyperfine fields in the 22–26-at.% Al region, led to a model in which the Fe moment was assumed[8-10] to vary with the number of nearest-neighbor Fe atoms n. In this model, it is generally assumed that the Fe moment remains at $2.2\mu_B$ for $n = 8$, 7, and 6 since the average moment of the disordered alloys out to 23-at.% Al decreases as for simple

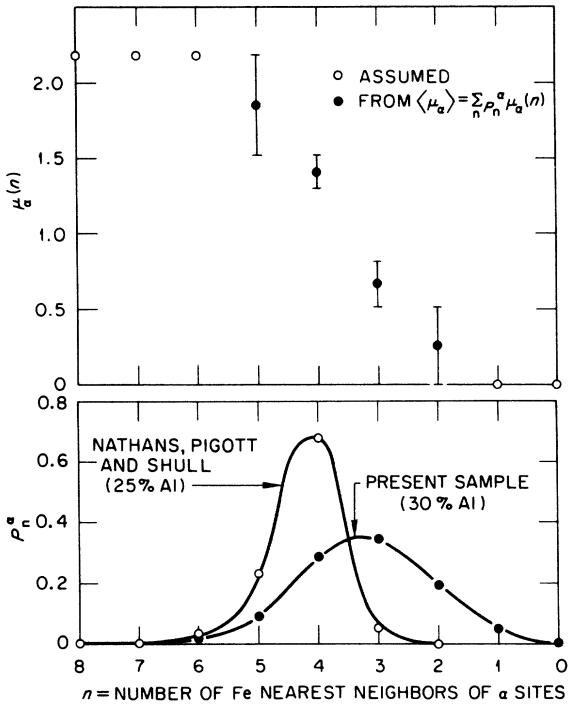

FIG. 4. P_n^α and $\mu_\alpha(n)$ for ordered Fe-Al alloys. The lower figure shows the probability distributions used to obtain the upper figure.

dilution. Also, since the 32–50-at.% Al alloys are paramagnetic, Fe atoms with $n=0$ and 1 are assumed to have no moment. This leaves only the $n=2$, 3, 4, and 5 cases to be assigned. The site occupation and site moment determinations for this 30-at.% alloy permit a refinement of the previous[8-10] assignments.

In this structure, the β sites have eight α-site nearest neighbors while the α sites have 4β- and 4γ-site nearest neighbors. Thus, the probability that a β site has n Fe nearest neighbors is

$$P_n^\beta = \binom{8}{n} r_\alpha^n (1-r_\alpha)^{8-n}, \tag{6}$$

while the probability that an α site has n Fe nearest neighbors is

$$P_n^\alpha = \sum_{l,m}^{l+m=n} P_l^{\beta\alpha} P_m^{\gamma\alpha}, \tag{7}$$

where

$$P_l^{\beta\alpha} = \binom{4}{l} r_\beta^l (1-r_\beta)^{4-l} \tag{8}$$

and

$$P_m^{\gamma\alpha} = \binom{4}{m} w_\gamma^m (1-w_\gamma)^{4-m}. \tag{9}$$

The P_n^α values of the two alloys considered for the moment assignment are shown in the lower part of Fig. 4. The average moments at the α and β sites are

$$\langle\mu_\alpha\rangle = \sum_n P_n^\alpha \mu_\alpha(n) \tag{10}$$

and

$$\langle\mu_\beta\rangle = \sum_n P_n^\beta \mu_\beta(n). \tag{11}$$

The 25-at.%-Al sample used by Nathans, Pigott, and Shull[1] had $r_\alpha=0.97$, $r_\beta=0.98$, $w_\gamma=0.08$, $\langle\mu_\alpha\rangle = 1.50\mu_B$, and $\langle\mu_\beta\rangle = 2.18\mu_B$ at 298 K. The present 30-at.%-Al alloy has $r_\alpha=1.00$, $r_\beta=0.70$, $w_\gamma=0.09$, and spontaneous moments $\langle\mu_\alpha\rangle = 0.324\mu_B$ and $\langle\mu_\beta\rangle = 0.780\mu_B$ at 220 K. With these r_α's both alloys have all β sites with $n\geq 6$ so that $\langle\mu_\beta\rangle$ should be the same for both samples. The smaller value observed for the 30-at.% alloy leads to the conclusion that only a fraction of this sample is spontaneously ferromagnetic. Since the diffuse-scattering data show the presence of ferromagnetic clusters, only a fraction of which are aligned by an applied field, we assume this is a volume effect and that only $0.780/2.18=0.358$ of the volume of the 30-at.% alloy is spontaneously ferromagnetic. Substitution of the volume corrected $\langle\mu_\alpha\rangle$ for the 30-at.% alloy and $\langle\mu_\alpha\rangle = 1.50\mu_B$ for the 25-at.% alloy into Eq. (10) with the restriction that

$$2.18 = \mu_\alpha(8) = \mu_\alpha(7) = \mu_\alpha(6) \geq \mu_\alpha(5) \geq \mu_\alpha(4) \geq \mu_\alpha(3) > \mu_\alpha(2) \geq 0$$

yields the moment assignment shown in the upper part of Fig. 4. This is in general agreement with the previous assignments, but should be better because of the larger $n=2$ and $n=3$ probabilities included here.

All of these assignments yield an unusually strong local environment effect for those configurations that occur with highest probability in the 25–32-at.%-Al region. We will use this dependence of μ_α on n and a ferromagnetic, nearest neighbor Fe_α-Fe_β interaction to account for the unusual magnetization behavior of this alloy. If there were regions of α-site Fe atoms with $n\geq 4$ and $n<4$, then the molecular fields at both α and β sites would be larger in the $n\geq 4$ regions because of the larger α-site moments and the larger number of β-site Fe atoms. The P_n^α distribution in Fig. 4 shows that 40% of the α sites have $n\geq 4$. One might therefore attribute the 36% by volume that is spontaneously ferromagnetic to these $\mathrm{Fe_3Al}$-like $n\geq 4$ regions and the remaining superparamagnetic volume to the $n<4$ regions. In fact, such regions do occur because of the sharing of β and γ sites by α sites so that any α site that has $n=4$ also has six α-site neighbors with a greater than average probability for $n=4$. For the same reason, an α site with $n<4$ is more likely to have neighboring

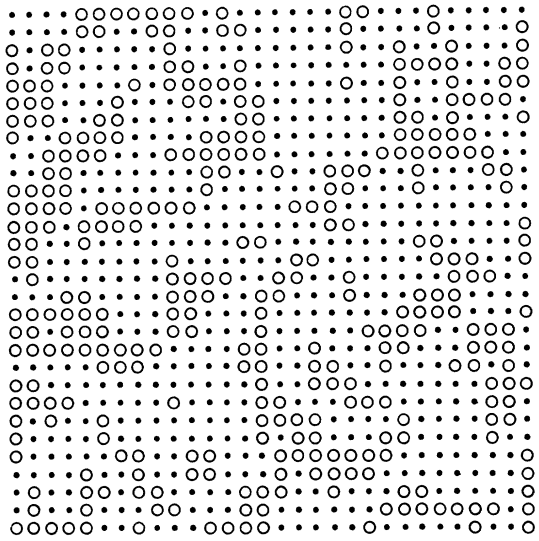

FIG. 5. A 30×30 array of α sites with $n \geq 4$ (open circles) and $n < 4$ (dots) showing evidence for clustering in the 30-at.%-Al alloy. This figure was obtained by a random filling of the surrounding β and γ sites in accordance with the known r_β and w_γ.

α sites with $n < 4$. As a result, the system tends to cluster into $n \geq 4$ and $n < 4$ regions. This clustering is illustrated in Fig. 5 which shows a 30 ×30 array of α sites in a (100) plane. The open circles indicate Fe atoms with $n \geq 4$ and the dots represent Fe atoms with $n < 4$. This array was obtained by filling the β and γ sites of the two adjacent (100) planes according to a random number program consistent with the known r_β and w_γ values, and then by finding n for each of the enclosed α sites. Even in this two-dimensional array, the clustering tendency is clearly evident.

Of course the three-dimensional picture is much more complicated. The concentration of $n \geq 4$ α sites is probably above the percolation concentration so that some of the clustered regions in Fig. 5 are already interconnected through tenuous percolation channels. Even so, the neutron-diffuse-scattering measurements would yield an average cluster size for the high-density $n \geq 4$ and $n < 4$ regions. The neutron results yield cluster diameters of approximately 25 Å, which corresponds to about nine grid spacings along the ⟨100⟩ directions in Fig. 5. The clustered regions in the figure are qualitatively consistent with this dimension.

The increasing antiferromagnetic tendencies with decreasing temperature may be caused by an antiferromagnetic interaction across the boundary between the two types of clusters. This might be an Fe_α-Fe_α interaction for those configurations without β-site Fe atoms in between or the 180° Fe_β-Al-Fe_β interaction assumed by Sato and Arrott.[11] The $n \geq 4$ regions with $\langle n \rangle = 4.30$ and $\langle \mu_\alpha \rangle = 1.54 \mu_B$ would presumably behave very much like stoichiometric Fe_3Al ($\sigma_{RT}/\sigma_0 = 0.88$) (Ref. 10) and have high relative magnetizations at room temperature. The $n < 4$ regions, however, have $\langle n \rangle = 2.48$ and $\langle \mu_\alpha \rangle = 0.47 \mu_B$ and would probably saturate at lower temperatures. On cooling, the increasing magnetization of the $n < 4$ regions would then cause an increase in the antiferromagnetic boundary interaction. This could destroy the ferromagnetic coupling in the interconnecting percolation channels of the $n \geq 4$ regions causing paramagnetism and, at lower temperatures, produce antiparallel alignment of the $n \geq 4$ and $n < 4$ regions.

Finally, we suggest that the rapid decrease in spontaneous magnetization with increasing Al content in this system is due to percolation of the $n \geq 4$ α sites. The sum of P_n^α for $n \geq 4$ decreases rapidly (from 0.95 at 25-at.% Al to 0.40 at 30-at.% Al) and approaches the site percolation concentration of 0.30 for a simple cubic lattice near the critical concentration (30.4-at.% Al) for ferromagnetism. It should be noted, however, that this percolation concentration of 0.30 is for random-site occupation while the $n \geq 4$ α-site occupation is not random but rather exhibits a pronounced short-range order. Unfortunately, the percolation problem with short-range order has not yet been treated so that a quantitative comparison with this percolation mechanism is not yet available.

ACKNOWLEDGMENTS

We wish to thank Professor P. A. Beck for suggesting this problem and for providing us with a carefully produced sample. Thanks are also due to T. Kaplan and M. Ulehla for discussion of the percolation problem and to J. Sellers for experimental assistance.

†Research sponsored by the ERDA under contract with Union Carbide Corp.

*Present address: Instituto Venezolano de Investigaciones Cientificas, Apartado 1827, Caracas, Venezuela.

[1]R. Nathans, M. T. Pigott, and C. G. Shull, J. Phys. Chem. Solids 6, 38 (1958).

[2]A. J. Bradley and A. H. Jay, Proc. R. Soc. Lond. A 136, 210 (1932).

[3]H. Okamoto and P. A. Beck, Met. Trans. 2, 569 (1971).

[4]A. Arrott and H. Sato, Phys. Rev. 114, 1420 (1959).

[5]R. D. Shull, H. Okamoto, and P. A. Beck, Solid State

Commun. 20, 863 (1976).
[6]We use the term "mictomagnetism" to denote a spin cancellation without the development of long-range order but in the presence of ferromagnetic short-range order.
[7]S. J. Pickart and R. Nathans, Phys. Rev. 123, 1163 (1961).
[8]E. A. Friedman and W. J. Nicholson, J. Appl. Phys. 34, 1048 (1963).
[9]P. A. Beck, Met. Trans. 2, 2015 (1971).
[10]H. Okamoto and P. A. Beck, Monatshifte F. Chemie 103, 907 (1972).
[11]H. Sato and A. Arrott, Phys. Rev. 114, 1427 (1959).